oxygen

MDPI

Article

Age-Related Expression and Localization of HIF-1α and HIF-2α in Different Tissues of Yak

Qin Wu [1,†], Huan Yang [1,†], Junyu Chen [1], Zhixin Chai [1], Hongwen Zhao [2,*] and Zhijuan Wu [1,*]

[1] College of Animal Husbandry and Veterinary Medicine, Southwest Minzu University, Chengdu 610041, China; wq202231301056@163.com (Q.W.); yh15719535013@163.com (H.Y.); chenjunyv2025@163.com (J.C.); chaizhixin2525@163.com (Z.C.)
[2] Sichuan Academy of Grassland Sciences, Chengdu 611731, China
* Correspondence: zhwdjc2014@163.com (H.Z.); wzjdream2005@163.com (Z.W.)
† These authors contributed equally to this work.

Abstract

The yak (*Bos grunniens*), a unique bovine species that is endemic to the Qinghai–Tibet Plateau and adjacent mountainous regions, exhibits remarkable adaptations to chronic high-altitude hypoxia. However, the molecular mechanisms underlying yaks' adaptation to this extreme environment remain poorly understood. This study aimed to elucidate the spatiotemporal expression dynamics of hypoxia-inducible factor 1α (HIF-1α) and 2α (HIF-2α) in major tissues of yaks across developmental stages (0.5, 1.5, 2.5, and 4.5 years; $n = 3$ per group). The tissues (heart, liver, spleen, lungs, kidneys, blood vessels and skeletal muscles) were analyzed using hematoxylin and eosin (H&E) staining and immunohistochemistry. The results revealed significant differences in the expression levels of HIF-1α and HIF-2α between tissues and at different ages. In cardiac tissue, both HIF-1α and HIF-2α are localized to the myocardial interstitium, with HIF-1α expression peaking at 1.5–2.5 years and HIF-2α expression reaching its maximum at 2.5 years. Hepatic HIF-1α showed perivenous hepatocytes enrichment and peaked at 2.5 years ($p < 0.01$ vs. other ages), while HIF-2α was uniformly distributed across lobules without age-related changes. Splenic HIF-1α and HIF-2α levels increased progressively with age, both peaking at 4.5 years ($p < 0.01$), and age was strongly correlated with expression levels (HIF-1α: r = 0.430; HIF-2α: r = 0.493). In pulmonary tissues, HIF-1α in bronchial smooth muscle peaked at 2.5 years, whereas alveolar septal HIF-2α peaked at 1.5 years ($p < 0.05$). In the kidney, HIF-1α was primarily localized to tubular epithelial cells and HIF-2α was diffusely distributed in the glomerular interstitium; neither factor showed significant variation across ages. In vascular tissues, HIF-1α expression remained stable across all ages and was predominantly observed in the smooth muscle layer, while HIF-2α exhibited a significant peak in endothelial cells at 2.5 years ($p < 0.01$). These findings suggest that HIF-1α predominates during early development stages, while HIF-2α becomes dominant as yaks approach maturity.

Keywords: yak; development; HIF-1α; HIF-2α

Check for updates

Academic Editors: Dong Uk Ahn and John T. Hancock

Received: 26 December 2025
Revised: 13 April 2026
Accepted: 25 April 2026
Published: 29 April 2026

Copyright: © 2026 by the authors. Licensee MDPI, Basel, Switzerland. This article is an open access article distributed under the terms and conditions of the Creative Commons Attribution (CC BY) license.

1. Introduction

The Qinghai–Tibet Plateau, spanning altitudes of 3000–5000 m, represents one of Earth's most extreme environments for both humans and wildlife, characterized by hypobaric hypoxia, frigid temperatures, intense ultraviolet radiation, sparse vegetation, and a truncated growing season [1]. Critically, these formidable conditions exert an irreplaceable

influence on the production systems and livelihoods of local pastoral and agricultural communities.

The yak (*Bos grunniens*), a unique large mammal that is endemic to the Qinghai–Tibet Plateau and its adjacent high-altitude regions, exhibits remarkable adaptability to high-altitude environments. At present, the number of yaks in our country is about 16 million [2], which is an important breed supporting the economic development of animal husbandry in the plateau area. High altitude environmental factors make yaks face severe survival challenges, such as hypoxia.

At the physiological structural level, yaks show increased alveolar area, elevated microvascular density, relatively enlarged cardiopulmonary volume, lifelong retention of fetal hemoglobin (HbF) with high oxygen affinity, and insensitivity to hypoxic pulmonary vasoconstriction, thereby avoiding pulmonary hypertension [1,3,4]. At the molecular and metabolic levels, the regulation of the hypoxia-inducible factor (HIF) signaling pathway, the positive selection of genes such as EPAS1/EGLN1 (endothelial PAS domain-containing protein 1/Egl-9 family hypoxia-inducible factor 1), optimization of mitochondrial oxidative phosphorylation efficiency, and reprogramming of glucose and lipid metabolism collectively enable efficient energy utilization and defense against oxidative damage under hypoxic conditions, forming a complete adaptive network from genotype to phenotype [5,6].

In particular, studies have suggested that the hypoxia signaling pathway and hypoxia-inducible factors play an important role in the hypoxia adaptation of yaks [1,7,8]. Xuebin Qi et al. conducted transcriptome analysis on the heart, liver, spleen, lung, kidney, muscle, testicle and brain tissue of yaks and found that multiple signaling pathways related to cell survival and proliferation, including HIF-1 signaling pathway, were significantly enriched [1]. By comparing the proteomic data of lung and heart tissue of high-altitude yaks and low-altitude ordinary cattle, Jinwei Xin et al. believe that HIF-1 signaling pathway is related to the hypoxic adaptive traits of yaks [8].

HIFs are central transcriptional regulators of the hypoxia signaling pathway, mediating cellular adaptation to oxygen deprivation. Functionally, HIFs exist as heterodimers composed of an oxygen-labile α subunit (HIF-α) and a constitutively expressed β subunit (HIF-1β). Among the three identified α subunit isoforms—HIF-1α, HIF-2α, and HIF-3α—HIF-1α and HIF-2α are the most extensively characterized, driving distinct transcriptional programs under hypoxic stress. Under a normal oxygen condition, the HIF-α subunit is degraded by proline hydroxylation through the ubiquitination pathway and cannot enter the nucleus. Under hypoxia conditions, HIF-α escapes the degradation pathway, enters the nucleus, binds to HIF-1β subunit to form HIFs heterodimers, and then binds to hypoxia response elements in the downstream gene promoter region to regulate the gene transcription [9].

In recent years, HIF-1α and HIF-2α have received much attention as key candidate genes for altitude hypoxia adaptation in humans and animals. Studies have shown that HIF-1α is an important regulatory factor in the hypoxia adaptation mechanism of reproductive activity in female yaks, and it is highly expressed in the granular layer of ovary and granular luteal cells [10]. The expression of Acyl-CoA Synthetase Short Chain Family Member 2 (ACSS2) gene in yak (high altitude) liver was significantly higher than that in Holstein cattle (low altitude); after deleting the ACSS2 gene from the yak fibroblast cell line, the mRNA expression of HIF-2α was significantly decreased [7].

Studies have shown that oxygen concentration also exerts a certain regulatory effect on the mRNA expression levels of HIF-1α and HIF-2α [11,12]. However, although the transcriptional activity of HIFs is related to their mRNA levels, it is mainly determined by the accumulation of HIF-α proteins and the formation of HIFα/β heterodimers, with subsequent nuclear translocation. Under normoxia, HIF-α subunits undergo rapid proteasomal

degradation via prolyl hydroxylation, whereas hypoxia stabilizes HIF-α proteins, enabling dimerization with HIF-1β to activate hypoxia-responsive genes [13]. This post-translational regulation implies that HIF mRNA levels poorly correlate with functional outputs, as evidenced by studies showing unchanged HIF-1α mRNA despite fluctuating protein levels under varying oxygen tensions [9,14]. Thus, protein-level analyses, as performed in this study, are essential to decipher HIF-mediated hypoxia adaptation.

Previous studies have suggested that HIF-1α and HIF-2α play a leading role in short-term (acute) and long-term (chronic) hypoxia stimulation conditions, respectively [13–16]. Specifically, HIF-1α dominates acute hypoxia responses by rapidly activating glycolytic enzymes (e.g., GLUT1, LDHA) and pro-survival genes to sustain ATP production, whereas HIF-2α orchestrates chronic adaptations through regulation of erythropoietin (EPO), vascular remodeling (VEGF), and iron metabolism (FPN1), ensuring systemic oxygen delivery and tissue homeostasis under prolonged hypoxia [14,15]. This functional dichotomy is further evidenced by temporal expression patterns: HIF-1α peaks within hours of hypoxia onset, while HIF-2α accumulates progressively over days to weeks [16].

Recent studies on the mechanism of hypoxia adaptation in humans and animals have found that both HIF-1α and HIF-2α have age-related persistent expression. Yanyu He et al. found that the expression level of HIF-1α protein showed significant age-related changes in the myocardial and coronary arteries of yaks: it increased significantly from 1 day old to 2 years old, and then decreased at 5 years old, with an extremely significant difference between the expression levels of HIF-1α at 1 day old and 2 years old [17]. However, the distinct expression dynamics and functional divergence between HIF-1 and HIF-2 during yak ontogeny, as well as their respective contributions to hypoxia adaptation, remain poorly characterized. Furthermore, studies on the protein expression localization and temporal changes in HIF-1α and HIF-2α in major yak tissues and organs during development are notably limited.

Critically, comparative analyses of HIF mRNA and protein levels between high-altitude yaks and low-altitude cattle may fail to accurately delineate HIFs' roles in yak development, due to confounding factors such as species-specific genetic backgrounds and environmental oxygen gradients [7]. For instance, cattle (e.g., Holsteins) exhibit distinct hypoxia-response thresholds compared to yaks, and HIF expression dynamics are further modulated by epigenetic adaptations to prolonged hypoxia [18]. In contrast, intra-population studies of yaks inhabiting the same high-altitude region allow for the precise dissection of developmental HIF expression patterns by minimizing environmental and interspecies variability [5].

In this study, the expression of HIF-1α and HIF-2α in major tissues and organs of yaks aged 0.5 years (late lactation stage, representing the initial state of hypoxia adaptation), 1.5 years (rapid growth phase, a window to test metabolic stress), 2.5 years (sexual maturity transition, facing endocrine and reproductive metabolic challenges), and 4.5 years (physical maturity, serving as a terminal reference baseline) was systematically analyzed via immunohistochemistry. These tissues and organs span six physiological systems: the circulatory (heart, blood vessels), respiratory (lung), metabolic (liver, kidney), immune (spleen), and muscular systems. This age gradient comprehensively covers the entire process of hypoxia adaptation from the initial establishment to terminal maturity, and this functional system-based profiling provides critical data to decipher how HIF isoforms coordinate hypoxia adaptation across distinct physiological niches during yak growth and development.

2. Materials and Methods

2.1. Experimental Materials

A total of 12 healthy male Maiwa yaks (3 per group) from four age groups (0.5, 1.5, 2.5, and 4.5 years old) were selected from the Qinghai–Tibet Plateau Ecological Protection and Animal Husbandry High-Tech Research Demonstration Base of Southwest Minzu University (elevation: 3600 m), Hongyuan County, Aba Tibetan and Qiang Autonomous Prefecture, Sichuan Province, China. The sample size (n = 3 per age group) was determined based on sample availability and literature precedence, as a similar immunohistochemical study in yaks also used three individuals per group [19]. Heart, liver, spleen, lung, kidney, blood vessels (collected from the aorta), and muscle tissues were collected from each yak, and fresh tissue samples (approximately 1 cm^3) were fixed in 4% paraformaldehyde for subsequent immunohistochemical analysis.

2.2. Hematoxylin-Eosin (H&E) Staining

The heart, liver, spleen, lung, kidney, and muscle tissues of yaks were embedded in paraffin, sliced into sections, and stained with hematoxylin for 4 min. The sections were then differentiated in 1% hydrochloric acid–alcohol solution (75% ethanol), rinsed with water, and then counterstained with 1% ammonia solution to restore the blue coloration. After washing, the sections were stained with eosin solution for 2 min, dehydrated through an ethanol series, cleared in xylene, and mounted with resin. The stained sections were examined under an Olympus CX31 optical microscope, and images were captured for histological analysis.

2.3. Immunohistochemistry (IHC)

Paraffin sections of yak tissues were subjected to heat-mediated antigen retrieval by being immersed in 1× citrate retrieval solution, heated in a microwave until boiling, maintained at sub-boiling temperature (95–98 °C) for 10 min, and cooled on the bench at room temperature for 30 min, then blocked with 5% goat serum for 30 min at room temperature. Primary antibodies that were pre-cooled to 4 °C were applied overnight in a humidified chamber: monoclonal mouse anti-HIF-1α (1:50 dilution; Invitrogen, Cat# MA1-16504) and polyclonal rabbit anti-HIF-2α (1:100 dilution; Invitrogen, Cat# PA1-16510). As a negative control, the isotype IgG was used instead of the primary antibody under the same conditions. Horseradish peroxidase (HRP)-conjugated goat anti-mouse/rabbit IgG (1:500 dilution; ZEN-BIO) was used as the secondary antibody and incubated at room temperature for 50 min. Chromogenic development was performed using freshly prepared DAB (Biosharp, Hefei, China) for 3–10 min under microscopic monitoring, and the reaction was terminated when optimal staining was achieved. Sections were then counterstained with hematoxylin. Sections were dehydrated, mounted, and imaged under a microscope. Six to seven random, non-overlapping high-power fields per section were photographed under consistent illumination and exposure settings. The positive expression area and cumulative optical density were quantified using Image-Pro Plus 5.1 software by observers who were blinded to the age groups.

2.4. Data Analysis

SPSS 26.0 software was used to perform one-way ANOVA, followed by Tukey's HSD post hoc test for multiple comparisons, and Pearson's correlation analysis. Prior to the analysis, the normality was assessed using the Shapiro–Wilk test and the linearity of the relationships was confirmed by a visual inspection of the scatter plots. A significance level of $\alpha = 0.05$ was adopted. Statistical graphs were prepared using GraphPad Prism 7.0. $p < 0.05$ was considered statistically significant, and $p < 0.01$ was considered highly significant.

Pearson correlation analysis was performed to evaluate linear relationships. The correlation strength was interpreted as follows: $|r| \leq 0.3$ indicated a weak correlation; $0.3 < |r| \leq 0.5$ indicated a moderate correlation; and $0.5 < |r| \leq 1.0$ indicated a strong correlation.

3. Results

3.1. Age-Dependent Histological Adaptations in Major Organs

Hematoxylin–eosin (H&E) staining revealed clear age-dependent morphological maturation across six major yak tissues (Figure 1). In the cardiac apex, myocardial fibers were loosely arranged with wide interstitial spaces at 0.5 and 1.5 years, became densely packed and uniformly aligned by 2.5 years, and maintained this organization at 4.5 years (Figure 1A–D). Hepatic lobules displayed loosely organized pericentral hepatocyte cords at 0.5 years, which progressively compacted into well-defined radial arrays by 2.5 years and remained consistent at 4.5 years (Figure 1E–H). The splenic white pulp density increased and splenic nodules and red pulp zones became more distinct from 0.5 to 4.5 years (Figure 1I–L). At 0.5 years of age, lung sections showed thickened alveolar septa and smaller airspaces, although the alveolar structures were less clearly resolved in younger animals (0.5 and 1.5 years) due to suboptimal image quality (Figure 1M,N). By 2.5 years, the alveoli were enlarged, the septal thickness became uniform and thin, and bronchial structures appeared more mature (Figure 1O). At 4.5 years, the alveolar septa were thicker than those at 2.5 years, while the overall alveolar morphology remained similar to that at 2.5 years (Figure 1P,O). Renal glomeruli and tubules matured from poorly differentiated structures at 0.5 years to well-organized glomerular tufts and densely lined tubular epithelia by 2.5 years, maintained at 4.5 years (Figure 1Q–T). Vascular walls showed progressive smooth muscle layer thickening across all ages from 0.5 to 4.5 years (Figure 1U–W). No inflammation, fibrosis, or other pathological alterations were observed in any tissue.

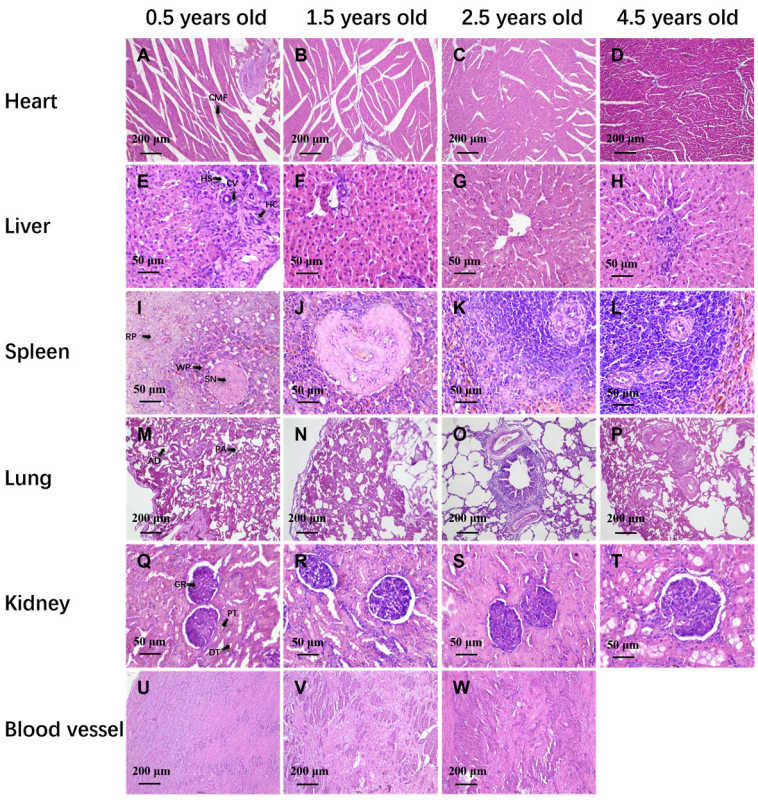


Figure 1. Hematoxylin–eosin staining of yak tissues. Representative images show the histological morphology of heart, liver, spleen, lung, kidney, and blood vessel of yaks at 0.5, 1.5, 2.5, and 4.5 years

of age (except blood vessel: 0.5, 1.5, 2.5 years only). (**A**–**D**) Heart; (**E**–**H**) liver; (**I**–**L**) spleen; (**M**–**P**) lung; (**Q**–**T**) kidney; and (**U**–**W**) blood vessel. Within each tissue, images from left to right represent ages in increasing order. Labeled structures: cardiac muscle fibers (CMF) in heart; hepatic cords (HC), hepatic sinusoids (HS), central vein (CV) in liver; splenic nodules (SN), white pulp (WP), red pulp (RP) in spleen; pulmonary alveoli (PA), alveolar duct (AD) in lung; and glomerulus (GR), proximal tubule (PT), distal tubule (DT) in kidney.

3.2. Age-Related Expression and Localization of HIF-1α in Different Tissues of Yaks

HIF-1α exhibited tissue-specific and age-dependent expression patterns, with generally higher expression in younger yaks (0.5–1.5 years) that declined with age, except in the liver, where expression increased again at 4.5 years. More specifically, in heart sections, HIF-1α localization was primarily cytoplasmic in cardiomyocytes; it was prominent at 0.5 years and decreased in intensity in older age groups, becoming nearly undetectable by 4.5 years (Figure 2A–D). In the liver, HIF-1α localization was confined to perivenous hepatocytes around the central veins and hepatic sinusoids; it was evident at 0.5 and 1.5 years, reduced at 2.5 years, and increased again by 4.5 years (Figure 2E–H). In the spleen, HIF-1α localization occurred in both white pulp follicles and red pulp cells, being moderate at 0.5 years, strongest in white pulp at 1.5 years, diminished by 2.5 years, and minimal at 4.5 years (Figure 2I–L). In lung tissue, HIF-1α localization was observed in bronchiolar and alveolar epithelial cells; it was weak at 0.5 years, strong at 1.5–2.5 years, and faint at 4.5 years (Figure 2M–P). In the kidney, HIF-1α localization appeared in glomerular and tubular cells, moderate at 0.5 years, absent in glomeruli at 1.5 years, and prominent in both compartments at 2.5 and 4.5 years (Figure 2Q–T). In blood vessels, HIF-1α localization was negligible across all age groups (Figure 2U–W).

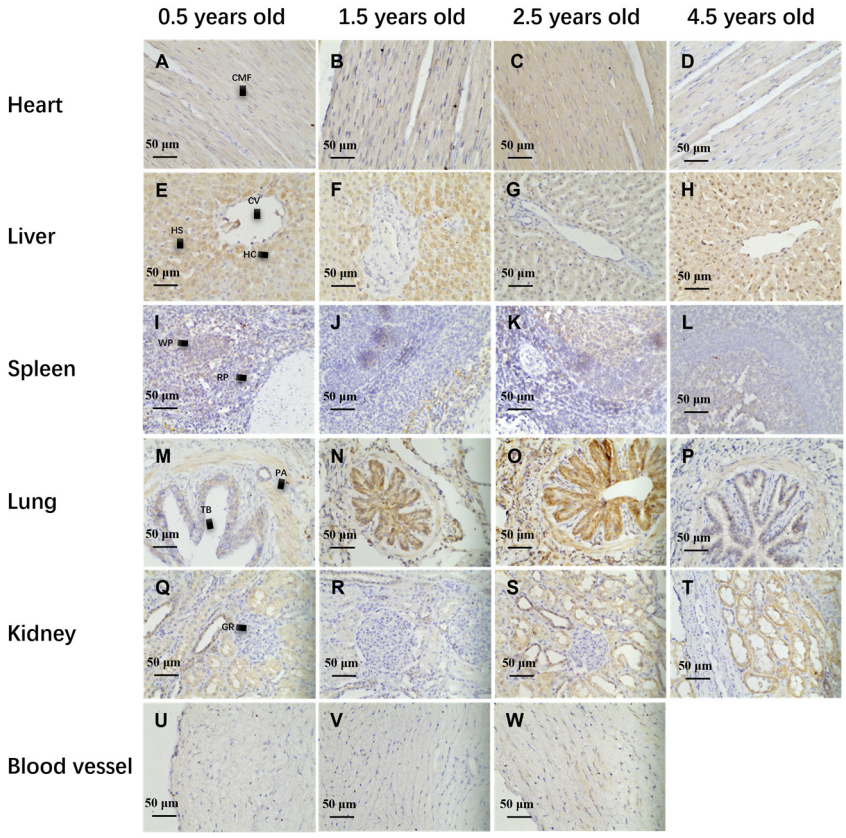


Figure 2. Expression and distribution of HIF-1α protein in yak tissues. Representative images show HIF-1α immunoreactivity (brown signal) in heart, liver, spleen, lung, kidney, and blood vessel of yaks

at 0.5, 1.5, 2.5, and 4.5 years of age (except blood vessels: 0.5, 1.5, 2.5 years only). (**A**–**D**) Heart; (**E**–**H**) liver; (**I**–**L**) spleen; (**M**–**P**) lung; (**Q**–**T**) kidney; and (**U**–**W**) blood vessels. Within each tissue, the images from left to right represent the ages in increasing order. Labeled structures: cardiac muscle fibers (CMF) in heart; hepatic cords (HC), hepatic sinusoids (HS), central vein (CV) in liver; white pulp (WP), red pulp (RP) in spleen; pulmonary alveoli (PA), terminal bronchiole (TB) in lung; and glomerulus (GR) in kidney. No specific labeling is shown for blood vessels due to negligible immunoreactivity.

3.3. Age-Related Expression and Localization of HIF-2α in Different Tissues of Yaks

HIF-2α showed tissue-specific and age-dependent expression, with peaks in the lung at 1.5–2.5 years and in the kidney at 2.5–4.5 years, but it declined with age in the heart and spleen and was negligible in blood vessels. Specifically, in the heart sections, HIF-2α localization in cardiomyocytes was observable at 0.5 years, yet its intensity diminished with advancing age, becoming less prominent in older groups (Figure 3A–D). In the liver, HIF-2α localization was restricted to perivenous hepatocytes around central veins and hepatic sinusoids, evident at 0.5 years, with a pattern that did not show a strict monotonic change across ages (Figure 3E–H). In the spleen, HIF-2α localization occurred in both white pulp and red pulp cells; it was moderate at 0.5 years, but the signal appeared to be less intense at subsequent ages, being minimal at 4.5 years (Figure 3I–L). In lung tissue, HIF-2α localization was seen in bronchiolar and alveolar regions, and was weak at 0.5 years, strong at 1.5–2.5 years, and faint at 4.5 years (Figure 3M–P). In the kidney, HIF-2α localization was present in glomerular and tubular cells, moderate at 0.5 years, and more prominent in both compartments at 2.5 and 4.5 years (Figure 3Q–T). In blood vessels, HIF-2α localization remained negligible across all age groups, with no significant signal detected (Figure 3U–W).

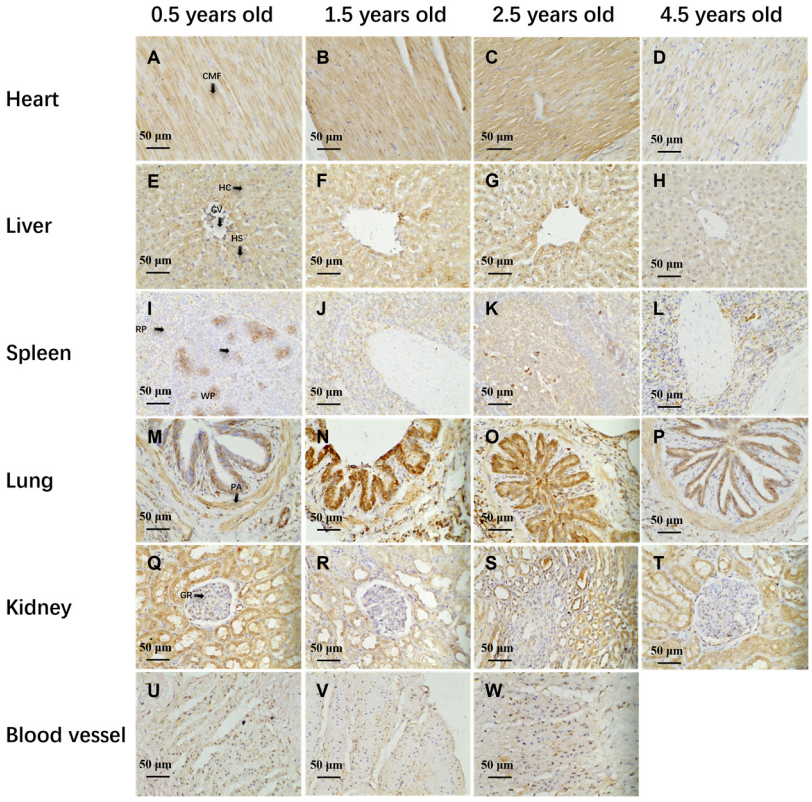


Figure 3. Expression and distribution of HIF-2α protein in yak tissues. Representative images show HIF-2α immunoreactivity (brown signal) in heart, liver, spleen, lung, kidney, and blood vessel of yaks

at 0.5, 1.5, 2.5, and 4.5 years of age (except blood vessels: 0.5, 1.5, 2.5 years only). (**A**–**D**) Heart; (**E**–**H**) liver; (**I**–**L**) spleen; (**M**–**P**) lung; (**Q**–**T**) kidney; and (**U**–**W**) blood vessel. Within each tissue, the images from left to right represent the ages in increasing order. Labeled structures: cardiac muscle fibers (CMF) in heart; hepatic cords (HC), hepatic sinusoids (HS), central vein (CV) in liver; white pulp (WP), red pulp (RP) in spleen; pulmonary alveoli (PA) in lung; and glomerulus (GR) in kidney. Vascular immunoreactivity was negligible; thus, no labeling is shown for blood vessels.

3.4. The Difference in HIF-1α and HIF-2α Expression Between Tissues in Yaks

Analysis of HIF-1α and HIF-2α expression levels in yaks (Figure 4) revealed age- and tissue-specific patterns. In 0.5-year-old yaks, HIF-1α expression was highest in the lung and blood vessels, with both significantly exceeding the levels in the spleen ($p < 0.05$), while HIF-2α expression peaked in the lung, followed by the kidney and blood vessels, with lung levels being significantly higher than those in the spleen and heart ($p < 0.01$), kidney levels surpassing the spleen and heart ($p < 0.05$), and blood vessel levels exceeding the spleen ($p < 0.05$) (Figure 4A). At 1.5 years of age, HIF-1α expression remained highest in blood vessels and the lung, which were both significantly elevated compared to the spleen ($p < 0.05$), and HIF-2α expression was also highest in the lung, followed by blood vessels, with the lung levels significantly exceeding the spleen ($p < 0.05$) (Figure 4B). In 2.5-year-old yaks, HIF-1α expression was highest in the lung but showed no significant inter-tissue differences, whereas HIF-2α expression remained lung-dominant, significantly surpassing the spleen and liver ($p < 0.05$) (Figure 4C). By 4.5 years of age, both HIF-1α and HIF-2α expression levels peaked in the spleen, with no significant differences observed across tissues (Figure 4D).

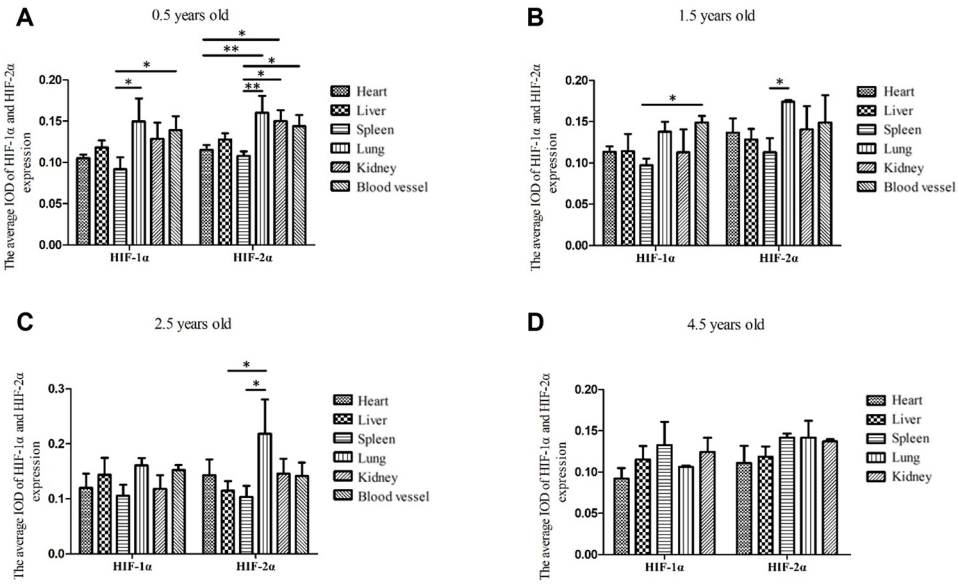


Figure 4. Differential expression of HIF-1α and HIF-2α proteins in yak tissues. Quantitative analysis of HIF-1α and HIF-2α expression in yak tissues at different ages was performed based on the IHC staining shown in Figures 2 and 3. The average integrated optical density (IOD) of HIF-1α and HIF-2α immunostaining is shown for four age groups: (**A**) 0.5 years, (**B**) 1.5 years, (**C**) 2.5 years, and (**D**) 4.5 years. Within each age group, the graphs compare protein expression levels among different tissues (heart, liver, spleen, lung, kidney, and blood vessel). For each tissue, six to seven random fields per section were photographed, and the positive expression area and cumulative optical density were quantified using Image-Pro Plus 5.1 software. Data are presented as mean ± SD ($n = 3$ per age group). Statistical significance is indicated as * $p < 0.05$ and ** $p < 0.01$ for comparisons among tissues within the same age group. The specific tissues and comparisons are detailed within each subpanel.

3.5. Age-Related Expression of HIF-1α and HIF-2α in Yaks

Analysis of age-related HIF-1α and HIF-2α expression in yaks (Figure 5) revealed tissue-specific developmental patterns. In the heart tissue, HIF-1α expression peaked at 1.5 years of age, followed by 2.5 years, with both stages showing significantly higher levels than at 4.5 years ($p < 0.01$ and $p < 0.05$, respectively), while the HIF-2α expression was highest at 2.5 years, significantly exceeding the levels at 0.5 and 4.5 years ($p < 0.01$) (Figure 5A). In the liver tissue, HIF-1α expression was maximal at 2.5 years, which was significantly elevated compared to 0.5, 1.5, and 4.5 years ($p < 0.01$), whereas HIF-2α levels showed no significant age-dependent variation (Figure 5B). Splenic HIF-1α and HIF-2α expression peaked at 4.5 years, with HIF-1α significantly elevated compared to 0.5, 1.5, and 2.5 years ($p < 0.05$–0.01) and HIF-2α exceeding all younger age groups ($p < 0.01$) (Figure 5C). Lung tissue exhibited maximal HIF-1α expression at 2.5 years, followed by 0.5 and 1.5 years, which were both significantly higher than at 4.5 years ($p < 0.01$ and $p < 0.05$, respectively), whereas HIF-2α expression peaked at 1.5 years, significantly exceeding the levels at 0.5 and 4.5 years ($p < 0.05$ and $p < 0.01$, respectively) and remaining higher than at 4.5 years in 2.5-year-old yaks ($p < 0.05$) (Figure 5D). No significant age-related differences were observed for either isoform in kidney tissues (Figure 5E). Vascular tissues showed stable HIF-1α expression across all ages, while HIF-2α levels peaked at 2.5 years, significantly surpassing 1.5-year-old yaks ($p < 0.01$) (Figure 5F).

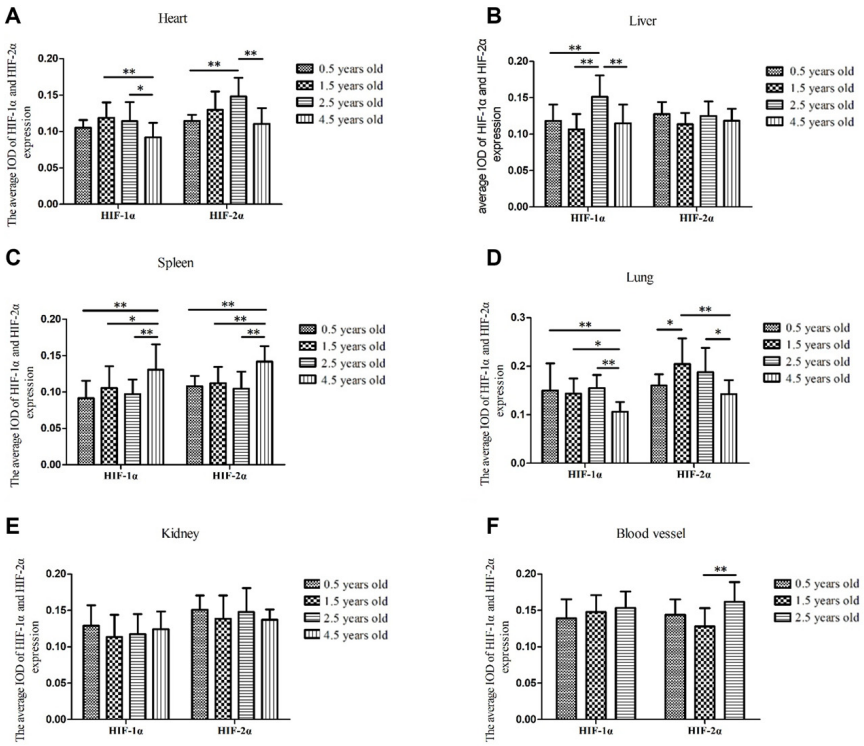


Figure 5. Differential expression of HIF-1α and HIF-2α proteins in yak tissues across ages. The average integrated optical density (IOD) of HIF-1α and HIF-2α immunostaining is shown for six tissues—heart, liver, spleen, lung, kidney, and blood vessel—based on the IHC staining shown in Figures 2 and 3. Tissue arrangement: (**A**) heart, (**B**) liver, (**C**) spleen, (**D**) lung, (**E**) kidney, and (**F**) blood vessel. Within each tissue, the bars compare the protein levels across the four age groups (0.5, 1.5, 2.5, and 4.5 years) for HIF-1α and HIF-2α separately. For each tissue, six to seven random fields per section were photographed, and the positive expression area and cumulative optical density were quantified using Image-Pro Plus 5.1 software. Data are presented as mean ± SD ($n = 3$ per age group). The statistical significance for comparisons between ages within the same protein is indicated as * $p < 0.05$ and ** $p < 0.01$ (as marked in the figure).

3.6. Correlation Analysis

In yak spleen, HIF-1α expression exhibited a moderate positive correlation with age ($r = 0.430$, $p < 0.01$), and HIF-2α expression showed a strong positive correlation ($r = 0.493$, $p < 0.01$). A moderate positive correlation was also observed between splenic HIF-1α and HIF-2α ($r = 0.310$, $p < 0.01$). In contrast, HIF-1α expression in yak lung demonstrated a moderate negative correlation with age ($r = -0.389$, $p < 0.01$), while HIF-2α expression displayed a weak negative correlation ($r = -0.249$, $p < 0.05$). Additionally, HIF-1α and HIF-2α expression in lung tissue were weakly positively correlated ($r = 0.277$, $p < 0.05$). All correlations are detailed in Table 1.

Table 1. Correlation analysis. Correlation analysis of age, HIF-1α and HIF-2α expression in different tissues (heart, liver, spleen, lung, kidney, and blood vessel).Values represent Pearson correlation coefficients (*r*). Correlation strength was interpreted as follows: $|r| \leq 0.3$ indicated a weak correlation; $0.3 < |r| \leq 0.5$ indicated a moderate correlation; and $0.5 < |r| \leq 1.0$ indicated a strong correlation. * $p < 0.05$ and ** $p < 0.01$ indicate statistically significant differences. HIF-1α, hypoxia-inducible factor 1α and HIF-2α, hypoxia-inducible factor 2α.

		Age	**HIF-1α**	**HIF-2α**
Heart	Age	1.000	0.021	−0.073
	HIF-1α	0.021	1.000	0.201
	HIF-2α	−0.073	0.201	1.000
Liver	Age	1.000	0.056	−0.135
	HIF-1α	0.056	1.000	0.077
	HIF-2α	−0.135	0.077	1.000
Spleen	Age	1.000	0.430 **	0.493 **
	HIF-1α	0.430 **	1.000	0.310 **
	HIF-2α	0.493 **	0.310 **	1.000
Lung	Age	1.000	−0.389 **	−0.249 *
	HIF-1α	−0.389 **	1.000	0.277 *
	HIF-2α	−0.249 *	0.277 *	1.000
Kidney	Age	1.000	−0.011	−0.147
	HIF-1α	−0.011	1.000	0.116
	HIF-2α	−0.147	0.116	1.000
Blood vessel	Age	1.000	0.239	0.264
	HIF-1α	0.239	1.000	0.172
	HIF-2α	0.264	0.172	1.000

* $p < 0.05$ and ** $p < 0.01$.

4. Discussion

This study systematically maps the expression dynamics of the hypoxia-inducible factors HIF-1α and HIF-2α in yaks (*Bos grunniens*), identifying tissue-specific and age-stratified patterns that correlate with high-altitude hypoxia adaptation. Through immunohistochemical examination of major organs—including the heart, liver, spleen, lung, kidney, and vascular tissues—across developmental stages (0.5 to 4.5 years), we demonstrate that these isoforms exhibit distinct spatiotemporal expression profiles, reflecting their specialized roles in mediating short-term and long-term hypoxia responses. The findings not only align with prior studies on plateau-adapted species but also provide new data supporting the proposed molecular mechanisms underlying yaks' resilience to extreme environmental stress.

In the cardiovascular system, HIF-1α immunoreactivity was detected in myocardial interstitial spaces and vascular smooth muscle layers, with relatively higher HIF-1α expression observed at 1.5–2.5 years of age. However, the staining signal in the heart was weak, which precluded definitive subcellular localization. Nonetheless, this transient

upregulation might be associated with the regulation of vascular tone and myocardial oxygen supply, potentially contributing to the metabolic demands of rapid growth under hypoxia in juvenile yaks. These observations resonate with studies on Gannan yaks, where HIF-1α overexpression in cardiac tissue was linked to improved hypoxia tolerance compared to low-altitude cattle [17,20,21]. In contrast, HIF-2α demonstrated stable expression in vascular endothelial cells across all age groups, suggesting a constitutive role in maintaining vascular integrity and long-term oxygen homeostasis. This dichotomy mirrors findings in murine models, where HIF-2α deficiency exacerbated hypoxia-induced pulmonary vascular remodeling [22], while HIF-1α-driven angiogenesis dominated acute responses [23].

The respiratory system further highlighted the functional divergence between HIF isoforms. In the lung tissue, HIF-1α was predominantly localized to the smooth muscle of terminal bronchioles and alveolar ducts during juvenile stages (0.5–2.5 years), coinciding with active airway development and hypoxic vasoconstriction. This transient expression pattern aligns with reports in Tibetan antelope, where HIF-1α levels in the lung significantly exceeded those in low-altitude relatives, facilitating rapid acclimatization [24]. Conversely, HIF-2α displayed sustained expression in alveolar septa and vascular walls: regions that are critical for gas exchange and chronic vascular adaptation. Such compartmentalization parallels observations in Magang geese, where HIF-2α's stability in pulmonary tissues supported long-term hypoxic endurance [25]. The age-dependent decline in HIF-1α in the lungs after 2.5 years, in contrast to HIF-2α's gradual accumulation, underscores a transition from short-term metabolic adjustments to sustained oxygen homeostasis—a strategy that is likely conserved across high-altitude species. Meanwhile, the observed changes in the pulmonary alveolar morphology, particularly the thickening of the alveolar septa at 4.5 years compared to 2.5 years, may reflect age-related structural remodeling of the lung under high-altitude conditions. Such remodeling could influence the gas exchange efficiency and oxygen diffusion capacity. Interestingly, the timing of septal thickening coincides with the shift from HIF-1α to HIF-2α dominance in lung tissue, suggesting a possible link between HIF-2α upregulation and alveolar structural maturation. However, this hypothesis requires further functional investigation.

In metabolic organs such as the liver and kidneys, HIF-1α and HIF-2α exhibited zonal specialization that was reflective of their distinct regulatory roles. Hepatic HIF-1α was predominantly localized to perivenous hepatocytes, regions characterized by lower oxygen tension, with expression intensifying progressively with age. This spatial and temporal pattern suggests a role in hypoxia-driven metabolic reprogramming, such as the upregulation of glycolysis and fatty acid oxidation pathways, as demonstrated in Maiwa yaks [26]. The preferential activation of HIF-1α in these oxygen-deprived zones likely enhances hepatic energy production under chronic hypoxia: a mechanism that is further supported by its interaction with PDK1-mediated mitochondrial regulation [27–29]. In contrast, HIF-2α's broad distribution across hepatic lobules—spanning the periportal to centrilobular regions—suggests a possible involvement in the redox balance and detoxification processes during prolonged oxygen scarcity. Renal tissues mirrored this functional division. HIF-1α's robust expression in tubular epithelial cells, escalating with age, aligns with its involvement in acute hypoxia sensing and electrolyte regulation. This finding corroborates studies in plateau myospalax, where renal HIF-1α mRNA levels surpassed those of other organs, highlighting its sensitivity to hypoxic stress [30]. HIF-2α, however, displayed a stable presence in the glomerular and interstitial regions, suggesting a role in long-term osmoregulation and erythropoietin (EPO) production—a hypothesis supported by its established regulation of EPO in murine models [31]. The coexistence of these iso-

forms in the kidney illustrates a layered adaptive strategy: HIF-1α addresses immediate oxygen deficits, while HIF-2α ensures sustained metabolic and hematopoietic stability.

The spleen emerged as a unique hub for hypoxia-mediated immune regulation. Both HIF-1α and HIF-2α expression increased with age, yet their spatial segregation—HIF-1α in white pulp lymphocytes versus HIF-2α in red pulp macrophages—implies specialized roles in immune adaptation. HIF-1α's concentration in lymphoid regions may drive hypoxia-induced hematopoiesis and lymphocyte proliferation, as observed in domestic yaks [32], while HIF-2α's red pulp dominance could modulate macrophage activity and iron recycling under chronic hypoxia. This compartmentalization aligns with broader mammalian immune mechanisms, where HIF-1α prioritizes acute inflammatory responses and HIF-2α supports anti-inflammatory resolution [33,34]. Developmental trajectories further reinforced the isoforms' complementary roles. HIF-1α peaked transiently in juvenile organs (e.g., lung, heart) that were critical for early survival, then declined as maturation reduced reliance on rapid metabolic adjustments. Conversely, HIF-2α's progressive accumulation in spleen and kidney—reaching maximal levels at 4.5 years—reflects its importance in maintaining homeostasis during adulthood: a pattern that is consistent with human studies where HIF-2α expression remained stable under prolonged hypoxia [35]. Vascular tissues epitomized this temporal hierarchy: HIF-1α's early dominance in smooth muscle facilitated juvenile vascular remodeling, while HIF-2α's endothelial persistence ensured lifelong vascular integrity.

It is worth noting that intestinal HIF-2α plays a central role in systemic iron homeostasis and erythropoiesis under hypoxic conditions. Intestinal HIF-2α upregulates key iron transporters (e.g., DMT1 and ferroportin), thereby enhancing dietary iron absorption. Together with renal HIF-2α-mediated erythropoietin (EPO) production, this forms a liver–intestine–kidney crosstalk that coordinates the iron supply and red blood cell production to maintain oxygen delivery [36,37]. Recent studies have shown that high-altitude hypoxia upregulates intestinal HIF-2α and its downstream iron-related genes, and that inhibition of intestinal HIF-2α alleviates excessive erythrocytosis [38,39]. Although we did not examine intestinal tissues in the present study, the age-related increase in HIF-2α expression observed in the lung, heart and liver suggests a possible systemic coordination with intestinal HIF-2α during yaks' development. Future studies integrating multiple organs, including the intestine, are needed to fully understand the systemic oxygen-sensing network.

The biphasic HIF regulatory framework observed in yaks—HIF-1α for immediate adaptation and HIF-2α for sustained homeostasis—likely represents an evolutionary convergence among high-altitude species. Tibetan antelope and sheep exhibit analogous HIF-1α lung specialization [24,40], while plateau rodents share renal HIF-2α conservation [30], suggesting universal principles of hypoxic resilience. Clinically, these insights could inform therapeutic strategies for altitude-related pathologies. For instance, augmenting HIF-1α activity might benefit individuals undergoing rapid ascent, whereas stabilizing HIF-2α could mitigate chronic mountain sickness. Moreover, the interplay between HIF isoforms and downstream targets like VEGF, PDK1, and EPO [27–29] highlights potential biomarkers for hypoxia adaptation. Future research should explore epigenetic and post-translational modifications regulating HIF stability, as well as cross-talk with other hypoxia-responsive pathways (e.g., NF-κB, mTOR). Such investigations could unlock novel interventions for ischemic diseases, leveraging lessons from yak adaptation.

Several limitations of this study should be acknowledged. First, the sample size (n = 3 per age group) is relatively small, limiting the statistical power and generalizability; as an exploratory descriptive study, our findings should be interpreted cautiously, with future larger cohorts needed to confirm trends. Second, the lack of fresh frozen tissue precluded Western blotting or immunofluorescence validation of IHC signals, rendering quantitative

protein expression interpretation preliminary. Third, we did not examine intestinal tissues, where HIF-2α plays a critical role in systemic iron metabolism and erythropoiesis. The potential contribution of intestinal HIF-2α to the observed systemic patterns therefore remains unknown. Finally, all animals were from a single high-altitude region, and yaks from different altitude levels were not selected for comparison; therefore, the results can only indicate the differences in HIF-1α and HIF-2α expression levels during the growth and development of yaks under high-altitude hypoxic conditions, but cannot be directly used to explain the hypoxia adaptation of yaks. Future studies may collect yak populations from different altitude levels for comparison to directly analyze the relationship between HIF expression and hypoxia adaptation. Despite these limitations, the study provides a preliminary systematic description of age-related HIF-1α and HIF-2α expression patterns in different yak tissues under high-altitude conditions, offering valuable clues for further exploring the mechanism of hypoxia adaptation in yaks.

Author Contributions: Q.W. and H.Y. contributed equally to this work as co-first authors: Conceptualization, Methodology, Investigation, Formal analysis, Writing—Original Draft. J.C.: Data curation, Validation. Z.C.: Formal analysis, Visualization. H.Z. and Z.W. (corresponding authors): Supervision, Funding acquisition, Project administration, Writing—Review and Editing. All authors have read and agreed to the published version of the manuscript.

Funding: The study was supported by (1) the Fundamental Research Funds for the Central Universities, Southwest Minzu University (Grant No: ZYN2025087), (2) the Qinghai Province Recount and Transformation Program (Grant No. 2023-QY-216), and (3) the Qinghai Science and Technology Major Program (Grant No. 2021-NK-A5).

Institutional Review Board Statement: This study was approved by the Animal Ethics Committee of Southwest Minzu University (Approval No. SMU-202501128, date of approval 15 May 2025). All animal procedures involved in the slaughter and sample collection were conducted in strict accordance with international animal welfare and ethical guidelines to minimize animal distress.

Data Availability Statement: The data presented in this study are available on request from the corresponding author due to the fact that the raw data are stored in the laboratory and not publicly archived.

Acknowledgments: The authors thank Southwest Minzu University, Key Laboratory of Qinghai-Tibetan Plateau Animal Genetic Resources, Ministry of Education, for providing the experimental platform and conditions.

Conflicts of Interest: These authors declare that they have no conflicts of interest.

References

1. Qi, X.; Zhang, Q.; He, Y.; Yang, L.; Zhang, X.; Shi, P.; Yang, L.; Liu, Z.; Zhang, F.; Liu, F.; et al. The Transcriptomic Landscape of Yaks Reveals Molecular Pathways for High Altitude Adaptation. *Genome Biol. Evol.* **2019**, *11*, 72–85. [CrossRef] [PubMed]
2. Sun, W.; Luo, Y.; Wang, D.H.; Kothapalli, K.S.D.; Brenna, J.T. Branched Chain Fatty Acid Composition of Yak Milk and Manure During Full-Lactation and Half-Lactation. *Prostaglandins Leukot. Essent. Fat. Acids* **2019**, *150*, 16–20. [CrossRef] [PubMed]
3. Liu, X.; Zhang, X. Transcriptomic and Metabolomic Insights into Age-Related Changes in Lung Tissue of Yaks under Highland Stress. *Int. J. Mol. Sci.* **2024**, *25*, 12071. [CrossRef]
4. Cui, C.; Chen, S.; Mi, B.; Qi, Y.; Jiao, C.; Zhang, M.; Dai, Y.; Wang, X.; Hu, J.; Shi, B.; et al. The Adaptive Strategies of Yaks to Live in the Asian Highlands. *Anim. Nutr.* **2022**, *9*, 249–258. [CrossRef] [PubMed]
5. Shahid, M.W.; Qaiser, H.; Hussain, T. Hypoxia Adaptation in Yak: Molecular, Genetic, and Physiological Mechanisms of High-Altitude Resilience. *Livest. Sci.* **2026**, *307*, 105921. [CrossRef]
6. Wang, B.; He, J.; Cui, Y.; Yu, S.; Zhang, H.; Wei, P.; Zhang, Q. The HIF-1α/EGF/EGFR Signaling Pathway Facilitates the Proliferation of Yak Alveolar Type II Epithelial Cells in Hypoxic Conditions. *Int. J. Mol. Sci.* **2024**, *25*, 1442. [CrossRef]
7. Wang, X.; Ju, Z.; Jiang, Q.; Zhong, J.; Liu, C.; Wang, J.; Hoff, J.L.; Schnabel, R.D.; Zhao, H.; Gao, Y.; et al. Introgression, admixture, and selection facilitate genetic adaptation to high-altitude environments in cattle. *Genomics* **2021**, *113*, 1491–1503. [CrossRef]

8. Xin, J.W.; Chai, Z.X.; Zhang, C.F.; Zhang, Q.; Zhu, Y.; Cao, H.W.; YangJi, C.; Chen, X.Y.; Jiang, H.; Zhong, J.C.; et al. Differences in Proteomic Profiles Between Yak and Three Cattle Strains Provide Insights into Molecular Mechanisms Underlying High-Altitude Adaptation. *J. Anim. Physiol. Anim. Nutr.* **2022**, *106*, 485–493. [CrossRef]
9. Wu, Z.; Zhang, W.; Kang, Y.J. Copper affects the binding of HIF-1α to the critical motifs of its target genes. *Metallomics* **2019**, *11*, 429–438. [CrossRef]
10. Fan, J.; Yu, Y.; Han, X.; He, H.; Luo, Y.; Yu, S.; Cui, Y.; Xu, G.; Wang, L.; Pan, Y. The expression of hypoxia-inducible factor-1 alpha in primary reproductive organs of the female yak (*Bos grunniens*) at different reproductive stages. *Reprod. Domest. Anim.* **2020**, *55*, 1371–1382. [CrossRef]
11. Xiong, X.; Fu, M.; Lan, D.; Li, J.; Zi, X.; Zhong, J. Yak Response to High-Altitude Hypoxic Stress by Altering mRNA Expression and DNA Methylation of Hypoxia-Inducible Factors. *Anim. Biotechnol.* **2015**, *26*, 222–229. [CrossRef] [PubMed]
12. Prabhakar, N.R.; Semenza, G.L. Adaptive and Maladaptive Cardiorespiratory Responses to Continuous and Intermittent Hypoxia Mediated by Hypoxia-Inducible Factors 1 and 2. *Physiol. Rev.* **2012**, *92*, 967–1003. [CrossRef]
13. Semenza, G.L. Hypoxia-Inducible Factors in Physiology and Medicine. *Cell* **2012**, *148*, 399–408. [CrossRef]
14. Keith, B.; Simon, M.C. Hypoxia-Inducible Factors, Stem Cells, and Cancer. *Cell* **2007**, *129*, 465–472. [CrossRef]
15. Wang, G.L.; Jiang, B.H.; Rue, E.A.; Semenza, G.L. Hypoxia-Inducible Factor 1 Is a Basic-Helix-Loop-Helix-PAS Heterodimer Regulated by Cellular O_2 Tension. *Proc. Natl. Acad. Sci. USA* **1995**, *92*, 5510–5514. [CrossRef]
16. Hu, C.J.; Wang, L.Y.; Chodosh, L.A.; Keith, B.; Simon, M.C. Differential Roles of Hypoxia-Inducible Factor 1α (HIF-1α) and HIF-2α in Hypoxic Gene Regulation. *Mol. Cell. Biol.* **2003**, *23*, 9361–9374. [CrossRef] [PubMed]
17. He, Y.; Yu, S.; Hu, J.; Cui, Y.; Liu, P. Changes in the Anatomic and Microscopic Structure and the Expression of HIF-1α and VEGF of the Yak Heart with Aging and Hypoxia. *PLoS ONE* **2016**, *11*, e0149947. [CrossRef] [PubMed]
18. Beall, C.M. Adaptation to High Altitude: Phenotypes and Genotypes. *Annu. Rev. Anthropol.* **2014**, *43*, 251–272. [CrossRef]
19. Zhang, Q.; Cui, Y.; Yu, S.; He, J.; Pan, Y.; Che, J. Proteomics and Expression of HIF2α/BNIP3L Signaling in Yak Brains at Different Altitudes. *Int. J. Mol. Sci.* **2025**, *26*, 1675. [CrossRef]
20. Urrutia, A.A.; Aragonés, J. HIF Oxygen Sensing Pathways in Lung Biology. *Biomedicines* **2018**, *6*, 68. [CrossRef]
21. He, Z.H.; Tian, M.; Wang, X.W.; Luo, X.; Tao, L.Q.; Zhao, Y.Q.; Ma, N.; Li, Z.Z. Association Between Metabolic Regulatory Enzymes and Hypoxia-Related Gene Expression in Yaks. *Mod. Anim. Husb. Vet. Med.* **2020**, *11*, 23–26. (In Chinese)
22. Cowburn, A.S.; Crosby, A.; Macias, D.; Branco, C.; Colaço, R.D.; Southwood, M.; Toshner, M.; Alexander, L.E.C.; Morrell, N.W.; Chilvers, E.R.; et al. HIF2α-Arginase Axis Is Essential for the Development of Pulmonary Hypertension. *Proc. Natl. Acad. Sci. USA* **2016**, *113*, 8801–8806. [CrossRef]
23. Raghavan, A.; Zhou, G.; Zhou, Q.; Ibe, J.C.; Ramchandran, R.; Yang, Q.; Racherla, H.; Raychaudhuri, P.; Raj, J.U. Hypoxia-Induced Pulmonary Arterial Smooth Muscle Cell Proliferation Is Controlled by Forkhead Box M1. *Am. J. Respir. Cell Mol. Biol.* **2012**, *46*, 431–436. [CrossRef] [PubMed]
24. Liu, F.; Wu, R.T.; Ma, L.; Yang, Y.Z.; Ge, R.L. Cloning and Tissue Expression of Hypoxia-Inducible Factor 1α Gene in Tibetan Antelope. *Acta Physiol. Sin.* **2011**, *63*, 565–573. (In Chinese)
25. Wu, D.S.; Chen, S.J.; Yang, C.; Liao, W.L.; Peng, C.T.; Huang, Y.M.; Liu, W.J. Cloning and Tissue Expression Analysis of HIF-1α Gene in Goose. *J. Zhongkai Univ. Agric. Eng.* **2020**, *33*, 15–20. (In Chinese)
26. Bai, M.; Hu, M.J.; Yang, Y.X.; Zhao, W.S.; Jiang, M.F. Relationship Between Promoter Methylation Levels of Hypoxia-Adaptive Genes and Tissue-Specific Expression in Yaks. *Chin. J. Anim. Sci.* **2020**, *56*, 67–72. (In Chinese)
27. Zhang, H.; He, H.; Cui, Y.; Yu, S.; Li, S.; Afedo, S.Y.; Wang, Y.; Bai, X.; He, J. Regulatory Effects of HIF-1α and HO-1 in Hypoxia-Induced Proliferation of Pulmonary Arterial Smooth Muscle Cells in Yak. *Cell. Signal.* **2021**, *87*, 110140. [CrossRef]
28. Lee, P.; Chandel, N.S.; Simon, M.C. Cellular Adaptation to Hypoxia Through Hypoxia Inducible Factors and Beyond. *Nat. Rev. Mol. Cell Biol.* **2020**, *21*, 268–283. [CrossRef]
29. Seong, H.A.; Jung, H.; Choi, H.S.; Kim, K.T.; Ha, H. Regulation of Transforming Growth Factor-Beta Signaling and PDK1 Kinase Activity by Physical Interaction Between PDK1 and Serine-Threonine Kinase Receptor-Associated Protein. *J. Biol. Chem.* **2005**, *280*, 42897–42908. [CrossRef]
30. Zhang, J.M. Seasonal Expression of HIF-1α and HO-1 in Plateau Zokor Tissues. Master's Thesis, Qinghai University, Xining, China, 2007. (In Chinese)
31. Rankin, E.B.; Biju, M.P.; Liu, Q.; Unger, T.L.; Rha, J.; Johnson, R.S.; Simon, M.C.; Keith, B.; Haase, V.H. Hypoxia-Inducible Factor-2 (HIF-2) Regulates Hepatic Erythropoietin In Vivo. *J. Clin. Investig.* **2007**, *117*, 1068–1077. [CrossRef] [PubMed]
32. Wang, D.P.; Li, H.G.; Guo, S.C.; Yang, J.; Qi, D.L.; Zhao, X.Q. Tissue-Specific Expression of HIF-1α Gene in Domestic Yaks from Qinghai. *J. Anhui Agric. Sci.* **2007**, *29*, 9173–9175. (In Chinese)
33. Ju, C.; Colgan, S.P.; Eltzschig, H.K. Hypoxia-Inducible Factors as Molecular Targets for Liver Diseases. *J. Mol. Med.* **2016**, *94*, 613–627. [CrossRef]

34. Bani Hashemi, S.; Braun, J.; Bernhardt, W.M.; Rascher, W.; Dötsch, J.; Trollmann, R. HIF-1α Subunit and Vasoactive HIF-1-Dependent Genes Are Involved in Carbon Monoxide-Induced Cerebral Hypoxic Stress Response. *Eur. J. Appl. Physiol.* **2008**, *104*, 95–102. [CrossRef] [PubMed]
35. Lundby, C.; Pilegaard, H.; Andersen, J.L.; van Hall, G.; Sander, M.; Calbet, J.A.L. Acclimatization to 4100 m Does Not Change Capillary Density or mRNA Expression of Potential Angiogenesis Regulatory Factors in Human Skeletal Muscle. *J. Exp. Biol.* **2004**, *207*, 3865–3871. [CrossRef]
36. Mastrogiannaki, M.; Matak, P.; Keith, B.; Simon, M.C.; Vaulont, S. Hypoxia-Inducible Factor-2α Mediates the Adaptive Increase of Intestinal Ferroportin During Iron Deficiency in Mice. *Gastroenterology* **2011**, *140*, 2044–2055. [CrossRef]
37. Das, N.K.; Schwartz, A.J.; Sharma, A.; Mukherjee, A.; Shah, Y. Hepatic Hepcidin/Intestinal HIF-2α Axis Maintains Iron Absorption During Iron Deficiency and Overload. *J. Clin. Investig.* **2018**, *129*, 336–348. [CrossRef]
38. Duarte, T.L.; Talbot, N.P.; Drakesmith, H.; Frost, M.C.; Talbot, N.P. NRF2 and Hypoxia-Inducible Factors: Key Players in the Redox Control of Systemic Iron Homeostasis. *Antioxid. Redox Signal* **2021**, *35*, 433–452. [CrossRef] [PubMed]
39. Zhou, S.; Yan, J.; Song, K.; Ge, R.L. High-Altitude Hypoxia Induces Excessive Erythrocytosis in Mice via Upregulation of the Intestinal HIF2a/Iron-Metabolism Pathway. *Biomedicines* **2023**, *11*, 2992. [CrossRef]
40. He, Y.; Munday, J.S.; Perrott, M.; Wang, G.; Liu, X. Association of Age with the Expression of Hypoxia-Inducible Factors HIF-1α, HIF-2α, HIF-3α and VEGF in Lung and Heart of Tibetan Sheep. *Animals* **2019**, *9*, 673. [CrossRef]

Disclaimer/Publisher's Note: The statements, opinions and data contained in all publications are solely those of the individual author(s) and contributor(s) and not of MDPI and/or the editor(s). MDPI and/or the editor(s) disclaim responsibility for any injury to people or property resulting from any ideas, methods, instructions or products referred to in the content.